CORRELATION AFTER REFLECTION IN A QUANTUM SYSTEM

by

Ryan S. Browne

A thesis submitted to the Faculty and the Board of Trustees of the Colorado School of Mines in partial fulfillment of the requirements for the degree of Master of Science (Applied Physics).

Golden, Colorado

Date ____________________

Signed: ____________________
Ryan S. Browne

Signed: ____________________
Dr. Frank Kowalski
Thesis Advisor

Golden, Colorado

Date ____________________

Signed: ____________________
Dr. Thomas Furtak
Professor and Head
Department of Physics

ABSTRACT

Reflection of a microscopic non-zero rest mass particle from a macroscopic mirror generates two-particle interference from the incident and reflected particle substates and the associated mirror substates. This amplifies effects such as fringe spacing since they are essentially determined not by the mass of the macroscopic mirror but rather by the much smaller mass of the microscopic particle. Coherence can be transferred during reflection from the initial particle substate to the mirror substate. Interference of multiple such two-particle states is discussed. These effects could lead to extending measurements of the quantum-classical boundary to larger masses.

The possibility of non-simultaneous measurement of the positions of the particle and the mirror is also discussed. The joint probability density, which is a function both of the different positions and different times at which the particle and mirror are measured, is derived assuming that no interaction occurs between the measurement times. An analog of the Doppler shift for this correlated system is discussed along with interference of multiple such two-particle states.

TABLE OF CONTENTS

LIST OF FIGURES

CHAPTER 1

LITERATURE SURVEY/BACKGROUND

Correlation and interference distinguish quantum mechanics of point particles from classical mechanics of point particles. The boundary between these regimes [1, 2] continues to be an area of interest both in attempts to explain why quantum effects are difficult to measure on a macroscopic scale [3–7] and in attempts to measure quantum effects on a macroscopic object [8–10].

A number of methods have been demonstrated that create these interesting states at the mesoscopic level. Reflection measurement methods involve light interacting with stationary [11] and oscillating mirrors [12–14] and with microwaves interacting with an oscillating mirror [15]. Reflection of a photon from an oscillating mirror [16] and using a Bose Einstein condensate as a mirror from which photons reflect [17] have also been studied.

Another method to create these types of states first creates a superposition of internal states, such as an atom that is in a superposition of spin up and spin down states, and then use laser pulses that only affect one of the two spin states to create spatial separation between the two states. This will lead to a correlation in the measurements of the position of particle and its internal spin state. However, because the position state is tied inexorably with the internal state, the correlation of measurements is easily broken by measurements that should not otherwise determine position.

Rather than addressing practical issues of implementation in detail, our work focuses on illustrating two properties of this correlation: the “amplification” of these interference effects and the transfer of coherence between the incident particle and mirror after reflection.

We will not deal with either quantum decoherence or issues associated with quantum measurement. We are solely looking at the predictions of axiomatic quantum mechanics.

CHAPTER 2

SIMULTANEOUS MEASUREMENT OF PARTICLE AND MIRROR

In this paper, I consider a system composed of a particle reflecting from a mirror, and the correlation of measurements of their states following their interaction. Both the mirror and particle have non-zero rest mass and motion is in free space along one dimension with all states unbound. We can consider this system as described by a single wavefunction composed of two substates, one for each particle.

2.1 Theory: Energy Eigenstates

The particle and mirror's interaction is modeled as a delta function potential tied to the position of the mirror. The reflectivity of the delta function is changed to model different physical systems.

Because the potential is a delta function, Schrödinger's equation can be can be solved entirely in regimes where the particle and mirror are free particles, with added boundary conditions at the delta function. Thus, the simplest solution to Schrödinger's equation for this system is plane waves for both the particle and the mirror. Due to the the superposition principle and the linearity of Schrödinger's equation, we can then build more physically realizable solutions from sums of these harmonic wave solutions.

If the particle and mirror are initially in eigenstates of energy, the states after reflection will also be eigenstates of energy. The particle-mirror state before the particle reflects from the mirror will interfere with the particle-mirror state after reflection. This is similar to the one-particle standing wave interference of a harmonic electromagnetic wave reflecting from a stationary mirror [18]. However, correlation in this two-particle interference (with the mirror being the second "particle") is manifest as a coincidence rate, e.g. a correlation in the measurement of particle-mirror positions.

In what follows, the solution to the Schrödinger equation for a particle-mirror in an eigenstate of energy is derived with arbitrary masses m and M and initial velocities v and V respectively. The superposition principle is then used to determine interference for the particle-mirror wavegroup. Using laboratory coordinates for the center of mass of the particle and mirror, x_1 and x_2 respectively, we calculate the joint probability density for simultaneously measuring the particle and mirror at different spacial locations.

Before reflection, the Schrödinger equation for the non-interacting particle-mirror state is

$$(\hbar\partial^2_{x_1}/2m + \hbar\partial^2_{x_2}/2M + i\partial_t)\Psi = 0. \tag{2.1}$$

The particle-mirror system has been partitioned into particle and mirror substates with a solution given by

$$\Psi_0 \propto \exp[i(kx_1 - \frac{\hbar k^2}{2m}t + Kx_2 - \frac{\hbar K^2}{2M}t)], \tag{2.2}$$

where k and K are the wavevectors for the particle and mirror respectively, $k = mv/\hbar$ and $K = MV/\hbar$.

A wavegroup constructed from the uncorrelated particle-mirror state in Equation 2.2 then leads to predictions about the probability of simultaneously finding the particle at x_1 and mirror at x_2. These wavegroup substates are not correlated. Therefore a measurement of the particle position affects neither the time evolution of the wavegroup substate associated with the mirror nor introduces any spatial correlation of the particle and mirror positions.

The particle-mirror interaction is modeled as a moving delta function potential where reflection occurs at the center of mass of the mirror with the Schrödinger equation given by

$$(\hbar\partial^2_{x_1}/2m + \hbar\partial^2_{x_2}/2M + \beta\delta[x_1 - x_2] + i\partial_t)\Psi = 0 \tag{2.3}$$

and one factor of $\hbar$ is included into β (square brackets are used to indicate the argument of a function). The mirror reflectivity, related to β, goes to infinity for a lossless mirror.

The solution yields an energy eigenstate for the particle-mirror interaction, for which neither the particle nor the mirror is localized. A wavegroup constructed from such solutions is described below.

A separable solution to the two-particle Schrödinger equation results from a transformation to the center of mass and relative coordinates, which does not change the total energy. The transformed Schrödinger equation becomes

$$(\frac{\hbar\partial^2_{x_{cm}}}{2M_{tot}} + \frac{\hbar\partial^2_{x_{rel}}}{2\mu} + \beta\delta[x_{rel}] + i\partial_t)\Psi[x_{cm}, x_{rel}, t] = 0 \tag{2.4}$$

where $M_{tot} = m + M$, $\mu = mM/(m+M)$, $x_{cm} = (mx_1 + Mx_2)/M_{tot}$, and $x_{rel} = x_2 - x_1$. The solution of the transformed equation corresponding to eigenstates of energy has time dependence

$$\exp[i(E_{rel} + E_{cm})t], \tag{2.5}$$

where

$$E_{rel} + E_{cm} = (\hbar K)^2/(2M) + (\hbar k)^2/(2m). \tag{2.6}$$

This reduces the Schrödinger equation to two ordinary differential equations:

$$-\frac{\hbar}{2M_{tot}}\frac{d^2U[x_{cm}]}{dx^2_{cm}} = E_{cm}U[x_{cm}] \tag{2.7}$$

$$\frac{\hbar}{2\mu}\frac{d^2u[x_{rel}]}{dx^2_{rel}} + \beta\delta[x_{rel}] = E_{rel}u[x_{rel}]. \tag{2.8}$$

The particle-mirror solution must vanish at $x_1 = x_2$ to satisfy the boundary condition at the mirror and not exist for $x_{rel} < 0$ (or $x_1 > x_2$) since the particle cannot move through the mirror. In this transformed system, a solution can be constructed from the superposition of incident and "reflected" wavefunctions,

$$\Psi = (e^{i\phi_{in}} - e^{i\phi_{ref}})\theta[x_{rel}], \tag{2.9}$$

where $\theta[x_{rel}]$ is the unit step function. The only difference between the arguments of the two exponentials is the sign of the relative wavevector K_{rel}, which due to reflection in the relative coordinate is negative. That is,

$$\phi_{in/ref} = K_{cm}x_{cm} - \frac{\hbar K_{cm}^2}{2M_{tot}}t \pm K_{rel}x_{rel} - \frac{\hbar K_{rel}^2}{2\mu}t \ , \tag{2.10}$$

where initial velocities must allow reflection to occur.

The particle-mirror system has now been partitioned into center of mass and relative coordinate substates. This separable solution, for the two uncorrelated substates, can be used to construct a wavegroup whose substates yield uncorrelated wavegroups associated with the center of mass and relative coordinates. A measurement of the center of mass position affects neither the time evolution of the wavegroup associated with the relative motion nor introduces any correlation between the center of mass and relative positions.

While the energy and momentum of the center of mass substate are unaffected by reflection that is not the case for the relative substate where the relative wavevector changes sign upon reflection. Therefore, in this separable system interference of incident and reflected wavefunctions, determined by the probability density

$$\Psi\Psi^* = 4\sin^2[K_{rel}x_{rel}], \tag{2.11}$$

is associated only with the relative coordinate substate.

However, changing the partition from center of mass and relative substates into particle and mirror substates yields a correlated state. This provides a method of extending the quantum-classical boundary since interference of the incident and reflected particle substates results in interference of the associated mirror substates due to the particle-mirror correlation.

This change of substates is accomplished by substituting the particle-mirror coordinates for the relative and center of mass coordinates in the separable solution given by Equations 2.9 and 2.10. The transformation involves $K_{cm} = k + K$, $K_{rel} = (Mk - mK)/M_{tot}$, $x_{rel} =$

$x_2 - x_1$, and $x_{cm} = (mx_1 + Mx_2)/M_{tot}$. These constraints transform $e^{i\phi_{in}}$ in Equation 2.9 into Equation 2.2. Transformation of the energy component of each substate must be consistent with energy and momentum conservation in reflection. The energy of the reflected particle is given by $p_{ref}^2/(2m)$ with $p_{ref} = \hbar\partial\phi_{ref}/\partial x_1$. Similarly, the energy for the mirror is $P_{ref}^2/(2M)$ with $P_{ref} = \hbar\partial\phi_{ref}/\partial x_2$. Both of these energies and momenta are consistent with those of a classical particle reflecting from a moving mirror.

Interference of these incident and reflected wavefunctions in the particle and mirror substates is then determined by

$$\Psi\Psi^* = 4\sin^2[\frac{(mK - Mk)\{(x_1 - x_2)\}}{(m + M)}], \tag{2.12}$$

which is similar to the interference pattern obtained in the correlation between two particles produced in a momentum-conserving decay [19]. Another characteristic of this equation is the lack of interference if only the mirror or particle is measured while measurement of both results in a correlation of their positions. For example, the probability for detecting the particle without measuring the mirror is manifest as an integral of Equation 2.12 over the mirror coordinate [19] or given by the reduced density matrix obtained as a trace over the mirror coordinates [20]. This averages out the interference pattern. However, simultaneous measurement of the mirror and particle at different positions yields the interference predicted by Equation 2.12.

2.2 Amplification

Consider such a simultaneous measurement. For fixed x_1 and a microscopic particle reflecting from a macroscopic mirror, the approximation $m/M << 1$ leads to interference *for the macroscopic mirror* which varies from maximum to minimum through a distance

$$\Delta x_2 \approx \pi\hbar/(m(v - V)). \tag{2.13}$$

Similarly for fixed x_2 this approximation leads to interference *for the microscopic particle* which varies from maximum to minimum through a distance $\Delta x_1 = \Delta x_2$.

These results can be compared with those for single particle interference of the mirror traversing a double slit of spacing d and distance from the slits to the screen of L. In the far field, the fringe spacing on the screen is $\Delta z = 2\pi L\hbar/(MVd)$. For a macroscopic mass, interference yields an imperceptible fringe spacing for any realistic double slit spacing.

If we assume that the mirror has no initial velocity ($V = 0$), then the fringe spacing of the mirror scales as the de Broglie wavelenghth of the particle reflecting from it. Thermal atoms have de Broglie wavelengths on the order of 10pm. Atoms in Bose-Einstein condensates have can have de Broglie wavelengths on the order of 1μm. [10]

This "amplification" of the interference effect, $\Delta x_2/\Delta z$, proportional to the ratio of the mirror and particle masses is caused by the generation of two mirror substates: before and after reflection of the microscopic particle. The difference in energy and momentum between these mirror substates is determined by a commensurate difference in the particle substates and is a function only of the particle mass for $M/m \gg 1$. The maxima to minima distances in interference are therefore the same for the particle and mirror and depend predominately on the mass of the particle for large mirror mass.

2.3 Wavegroups

To better understand the experimental consequences of these results, wavegroups are next formed from a superposition of the incident and reflected harmonic states (given in Equation 2.9) expressed in terms of the correlated particle and mirror substates. An analytic expression for such wavegroups can be obtained for a Gaussian distribution of wavevector components k and K (e.g. for the mirror this is proportional to $\exp[-(K - K_0)^2]/(2\Delta K^2)$ where the peak of the distribution is at K_0 and ΔK its width). The incident wavegroup propagates in the (x_1, x_2) plane along a line whose slope is determined by a ratio of the group velocities of each substate and spreads due to dispersion independently in each direction.

2.4 Interference in Correlated Measurements

In Figure 2.1 snapshots of the two-particle probability density function are shown at three times for $M/m = 100$, $\Delta K/\Delta k = 2$, and $K/k = 60$. Inspection of these snapshots confirms that the spatial location of the interference maxima and minima do not depend on time as discussed above. Also, a slice of this figure, along x_2 for fixed x_1 shows the same fringe spacing as does an orthogonal slice, as discussed for the approximation $M/m >> 1$ following Equation 2.13. In the center of mass and relative coordinate system (not shown) the "fringes" are aligned parallel to the center of mass coordinate illustrating the result given in Equation 2.11.

The minima of the interference shown in Figure 2.1 correspond to positions where the particle and mirror can never simultaneously be found. This is independent of time as long as the incident and reflected wavefunctions overlap. Verification of this result requires simultaneous measurement of the particle and mirror with instruments which have a spatial resolution that is smaller than this fringe spacing along both coordinates.

A slice of Figure 2.1 for $x_1 = 0$ along the x_2 coordinate is shown in Figure 2.2 (the solid line) and confirms that a slice of this for $x_2 = 0$ along x_1 (the dashed line) shows essentially the same fringe spacing for narrow bandwidth wavegroups, as discussed for the approximation $M/m >> 1$ following Equation 3.10.

In the center of mass and relative coordinate system (not shown) the "fringes" are aligned parallel to the center of mass coordinate illustrating the result given in Equation 3.8. The minima of the interference shown in Figure 2.1 correspond to positions where the particle and mirror can never simultaneously be found. Verification of this result requires simultaneous measurement of the particle and mirror with instruments which have a spatial resolution that is smaller than this fringe spacing along both coordinates.

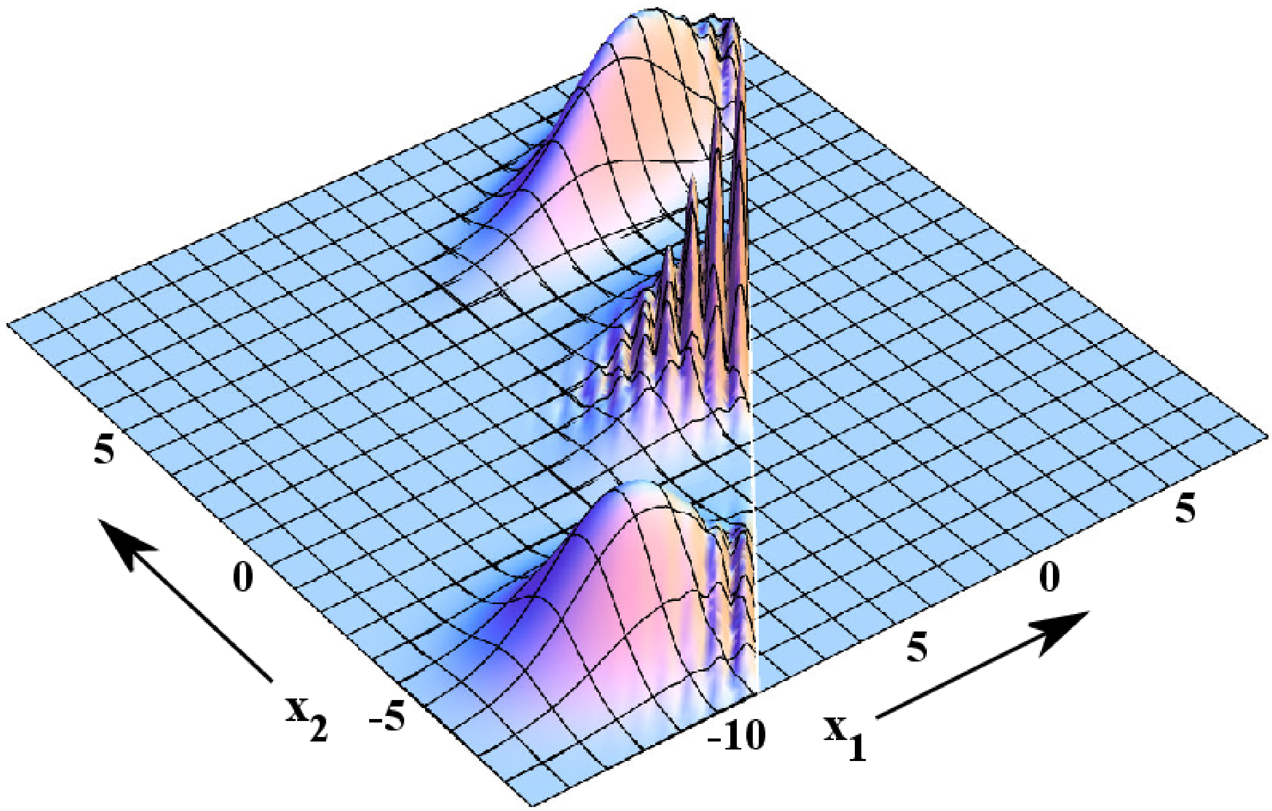

Figure 2.1: PDF plots of *simultaneous* snapshots for 3 sequential times vs coordinates (x_1, x_2). The lower wavegroup is moving toward the diagonal white line, corresponding to $x_1 = x_2$, then reflects from it in the middle snapshot where the incident and reflected two-particle wavefunctions overlap, and finally moves away from the diagonal in the upper snapshot.

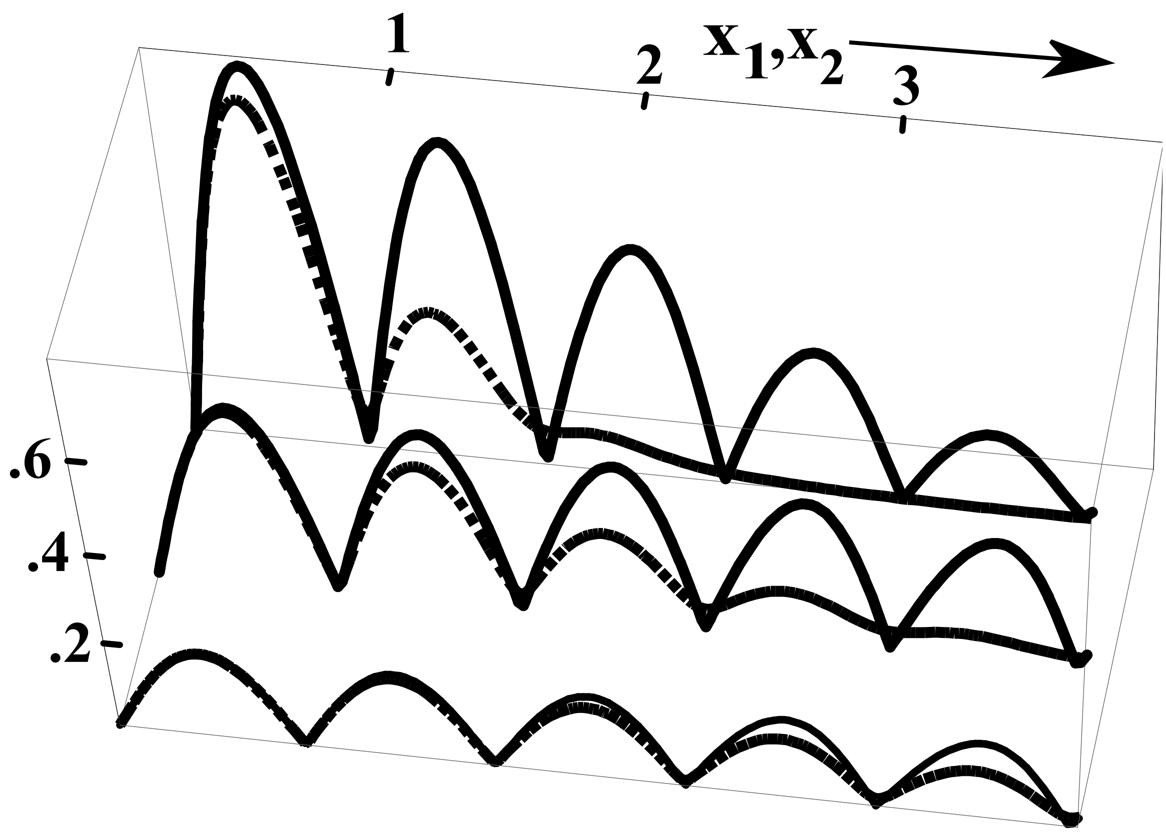

Figure 2.2: Slices of middle snapshot of Figure 2.1 along the x_2 axis for $x_1 = 0$ (dashed lines) and along the x_1 axis for $x_2 = 0$ (solid lines). The x_1 axis has been inverted to display both the dashed and solid lines together. Although each graph has $\Delta K/\Delta k = 2$ the value of ΔK decreases sequentially by a factor of 2 from back to front.

2.5 Comparison With Maxwell's Equations

It is important to take a moment, and relate these results to the results we would see if we considered this system from a more classical approach. Modeling this system with classical electromagnetism would result in standing wave interference in the light reflecting from the mirror. The mirror would also gain momentum from the light beam.

The solution in classical physics uses the position of the mirror as a boundary condition for Maxwell's equations, but the state of the mirror itself is not part of the solution to Maxwell's equations. In contrast, in this quantum mechanical scenario, the state of the mirror is explicitly part of the solution of the system, as well as the state of the particle reflecting from the mirror. This allows the state of the mirror to directly couple with the state of the reflected particle.

CHAPTER 3

NON-SIMULTANEOUS MEASUREMENT OF THE PARTICLE AND MIRROR

This work can be further generalized. Thus far, we have only considered measuring the position of the particle and mirror simultaneously. However, there are insights to be gained by looking at this system when the times of measurement are not simultaneous.

We propose that a description of such a system is given by a joint PDF which is a function both of the different particle positions and different times at which each is measured. This assumes that between the times of the two measurements there is no interaction.[21]

Such a prediction becomes non-trivial when the eigenstates of energy are superposed to form a particle-mirrror wavegroup. A measurement of the energy of the reflected particle substate then no longer leaves the reflected mirror substate with a unique energy since the interaction could have occurred between many different initial particle and mirror energy combinations from which the incident particle-mirror wavegroup was constructed. The focus here, however, is on how this is manifest in correlated measurements of the positions at different times of the particle and mirror.

We must again start construction of this wavegroup by solving the Schrödinger equation for a particle-mirror wavefunction in an eigenstate of energy.

The particle and mirror have arbitrary masses m and M and initial velocities v and V respectively. Laboratory coordinates are used for the center of mass of the particle and mirror, x_1 and x_2 respectively. The incident and reflected particle-mirror wavegroups interfere when they overlap. This is similar to the one-particle standing wave interference of a harmonic electromagnetic wave reflecting from a stationary mirror [18]. However, correlation results in two-particle interference which is manifest as a coincidence rate, i.e. a correlation in particle-mirror positions.

To account for different temporal measurements of the particle and mirror, respective time parameters t_1 and t_2 are introduced. These are used to identify the energies of the particle and the mirror in the expression for the wavefunctions total energy and to label the different times at which the particle and mirror are measured.[21] They neither tick at different rates nor are they out of phase.

3.1 Theory

This derivation proceeds as before, however, the total wavefunction is now a function of four parameters, two positions, x_1 and x_2 and two times t_1 and t_2.

Before reflection, the Schrödinger equation for the non-interacting particle-mirror state is

$$(\hbar(\partial_{x_1}^2/2m + \partial_{x_2}^2/2M) + i(\partial_{t_1} + \partial_{t_2}))\Psi = 0.$$

The particle-mirror system has been partitioned into particle and mirror subsystems. This notation provides a label to which the energy and wavevector of each object is associated, as is illustrated in the solution given by

$$\Psi_0 \propto \exp[i(kx_1 - \frac{\hbar k^2}{2m}t_1 + Kx_2 - \frac{\hbar K^2}{2M}t_2)], \tag{3.1}$$

where k and K are the wavevectors for the particle and mirror respectively, $k = mv/\hbar$ and $K = MV/\hbar$. A wavegroup constructed from the separable particle-mirror state in Equation 3.1 then leads to uncorrelated predictions about the probability of finding the particle at (x_1, t_1) and mirror at (x_2, t_2).

The particle-mirror interaction is modeled as a moving delta function potential where reflection occurs at the center of mass of the mirror with the Schrödinger equation given by

$$\begin{aligned}(\hbar\partial_{x_1}^2/2m + \hbar\partial_{x_2}^2/2M + \beta\delta[x_1 - x_2]\\ +i(\partial_{t_1} + \partial_{t_2}))\Psi[x_1, x_2, t_1, t_2] = 0,\end{aligned} \tag{3.2}$$

where one factor of $\hbar$ is included into β (square brackets are used to indicate the argument of a function). The mirror reflectivity, related to β, goes to infinity for a lossless mirror. Of interest is a solution which yields an energy eigenstate for the particle-mirror interaction, for which neither the particle nor the mirror is localized. A wavegroup constructed from such solutions is then described below.

A separable solution to this two-particle Schrödinger equation results from a transformation to the center of mass and relative coordinates x_{cm} and x_{rel} with respective energies E_{cm} and E_{rel}. This transformation does not change the total energy; $(\hbar K)^2/(2M)+(\hbar k)^2/(2m) = E_{rel} + E_{cm}$. Relative and center of mass times t_{rel} and t_{cm} are introduced and associated with the relative and center of mass energies. These time variables satisfy the same properties as t_1 and t_2 but in this case provide the notation needed in separating the energies associated with the relative and center of mass subsystems along the time coordinate while also facilitating calculations of each subsystem at different times.

The transformed Schrödinger equation becomes

$$\begin{aligned}&(\hbar\partial^2_{x_{cm}}/(2M_{tot}) + \hbar\partial^2_{x_{rel}}/(2\mu) + \beta\delta[x_{rel}]\\ &+i(\partial_{t_{cm}} + \partial_{t_{rel}}))\Psi[x_{cm}, x_{rel}, t_{cm}, t_{rel}] = 0,\end{aligned} \tag{3.3}$$

where $M_{tot} = m + M$, $\mu = mM/(m + M)$, $x_{cm} = (mx_1 + Mx_2)/M_{tot}$, and $x_{rel} = x_2 - x_1$. The solution of the transformed equation corresponding to eigenstates of energy has time dependence $\exp[i(E_{rel}t_{rel} + E_{cm}t_{cm})]$. This reduces the Schrödinger equation to two ordinary differential equations:

$$-\frac{\hbar}{2M_{tot}}\frac{d^2U[x_{cm}]}{dx^2_{cm}} = E_{cm}U[x_{cm}] \tag{3.4}$$

$$-\frac{\hbar}{2\mu}\frac{d^2u[x_{rel}]}{dx^2_{rel}} + \beta\delta[x_{rel}] = E_{rel}u[x_{rel}] \tag{3.5}$$

The particle-mirror solution must vanish at $x_1 = x_2$ to satisfy the boundary condition at the mirror and not exist for $x_{rel} < 0$ (or $x_1 > x_2$) since the particle cannot move through the mirror. In this transformed system, a solution can be constructed from the superposition of incident and "reflected" wavefunctions,

$$\Psi = (e^{i\phi_{in}} - e^{i\phi_{ref}})\theta[x_{rel}], \tag{3.6}$$

where $\theta[x_{rel}]$ is the unit step function. The only difference between the arguments of the two exponentials is the sign of the relative wavevector K_{rel} corresponding to reflection in the relative coordinate. That is,

$$\begin{aligned} \phi_{in/ref} = K_{cm}x_{cm} - \frac{\hbar K_{cm}^2}{2M_{tot}}t_{cm} \\ \pm K_{rel}x_{rel} - \frac{\hbar K_{rel}^2}{2\mu}t_{rel}, \end{aligned} \tag{3.7}$$

where the initial velocities must allow reflection to occur. The particle-mirror system has now been partitioned into separable center of mass and relative coordinate subsystems. This separable solution, for the two uncorrelated substates, can be used to construct a wavegroup whose substates yield uncorrelated wavegroups associated with the center of mass and relative coordinates. A measurement of the center of mass position affects neither the time evolution of the wavegroup associated with the relative motion nor introduces any correlation between the center of mass and relative positions.

While the energy and momentum of the center of mass subsystem are unaffected by reflection that is not the case for the relative subsystem where the relative wavevector changes sign upon reflection. Therefore, in this separable system interference of incident and reflected wavefunctions, determined by the PDF

$$\Psi\Psi^* = 4\sin^2[K_{rel}x_{rel}], \tag{3.8}$$

is associated only with the relative coordinate subsystem. However, partitioning the particle-mirror system into particle and mirror subsystems yields a correlated state.

This change of subsystems is accomplished by substituting the particle-mirror coordinates for the relative and center of mass coordinates in the separable solution given by Equations

3.6 and 3.7. The transformation involves: $K_{cm} = k + K$, $K_{rel} = (Mk - mK)/M_{tot}$, $x_{rel} = x_2 - x_1$, and $x_{cm} = (mx_1 + Mx_2)/M_{tot}$. Transformation of the temporal part of this solution, for this simple case of motion at constant speed, is constrained by the condition that the separation of the total energy into particle and mirror components must be consistent with energy and momentum conservation in reflection.

Application of this condition transforms $e^{i\phi_{in}}$ in Equation 3.6 (and the appropriately modified Equation 3.7) into Equation 3.1. The expression for $e^{i\phi_{ref}}$, although simple to calculate, is too large to present here. However, the energy of the reflected particle, given by $p_{ref}^2/2m$ with $p_{ref} = \hbar\partial\phi_{ref}/\partial x_1$, is associated with the temporal coordinate t_1. Similarly, the energy for the mirror is $P_{ref}^2/2M$ with $P_{ref} = \hbar\partial\phi_{ref}/\partial x_2$ and is associated with the temporal coordinate t_2. Both of these energies and momenta are consistent with those of a classical particle reflecting from a moving mirror.

Interference of these incident and reflected wavefunctions in the particle and mirror subsystems is then determined by

$$\begin{aligned}\Psi\Psi^* = 4\sin^2[&(mK - Mk)\{(m + M)(x_1 - x_2)\\ &-\hbar(k + K)(t_1 - t_2\}/(m + M)^2],\end{aligned} \tag{3.9}$$

which differs from the interference pattern obtained in the correlation between two particles produced in a momentum-conserving decay [19] predominately by the temporal factor for non-simultaneous measurement.

3.2 Discussion

To gain familiarity with this result, consider a simultaneous measurement. For fixed x_1, the approximation $m/M << 1$ leads to interference for the mirror which varies from maximum to minimum through a distance

$$\Delta x_2 \approx \pi\hbar/(m(v - V)). \tag{3.10}$$

Similarly for fixed x_2 this approximation leads to interference for the particle which varies from maximum to minimum through a distance $\Delta x_1 = \Delta x_2$, as has been seen in the case of simultaneous measurement.

Consider next the time dependence in Equation 3.9 which is determined by the time components of the phase of the incident wavefunction, $\Phi_{in}[t_1, t_2] = p_{in}^2 t_1/2m + P_{in}^2 t_2/2M$, and the reflected wavefunction, $\Phi_{ref}[t_1, t_2] = p_{ref}^2 t_1/2m + P_{ref}^2 t_2/2M$. The temporal part of the PDF depends on $\Phi_{in}[t_1, t_2] - \Phi_{ref}[t_1, t_2]$. For simultaneous measurements this phase difference is zero since the time variable factors from all energy terms and the total energy is invariant. That, however, is not the case for non-simultaneous measurements since time is no longer a common factor of all energy terms in the phase.

If x_1, x_2, and t_2 are fixed while t_1 is allowed to vary, the resulting time dependent interference pattern is the expected "beat frequency" $\Delta\Omega$ associated with interference of the incident and reflected particle substates (the superposition of states with different energies). If instead, x_1, x_2, and t_1 are fixed while t_2 is allowed to vary, the "beat frequency" that associated with superposing mirror substates differing in energy. These beat frequencies are identical due to the same energy being exchanged between the particle and mirror in reflection and are given by

$$\Delta\Omega = \frac{mM(v-V)(mv+MV)}{\hbar(m+M)^2} \approx \frac{m(v-V)V}{\hbar} \tag{3.11}$$

where the approximation is for $m/M << 1$. The approximate result is determined only by the particle mass.

3.3 Wavegroups

To better understand the experimental consequences of these results, wavegroups are next formed from a superposition of the incident and reflected harmonic states (given in Equation 3.6) expressed in terms of the particle and mirror subsystems. An analytic expression for such wavegroups can be obtained from a gaussian distribution of wavevector components k

and K (e.g. for the mirror this is proportional to $\exp[-(K-K_0)^2]/(2\Delta K^2)$ where the peak of the distribution is at K_0 and ΔK is the width).

3.4 Results

The "Doppler shift" for the mirror given in Equation 3.11 is illustrated for wavegroups by starting with a plot of a slice of Figure 2.1 for $x_1 = 0$ and $t_1 = t_2 = 0$ along the x_2 coordinate as the leftmost graph. Graphs toward the right progressively increase t_2 by 0.04τ while all other parameters remain fixed.

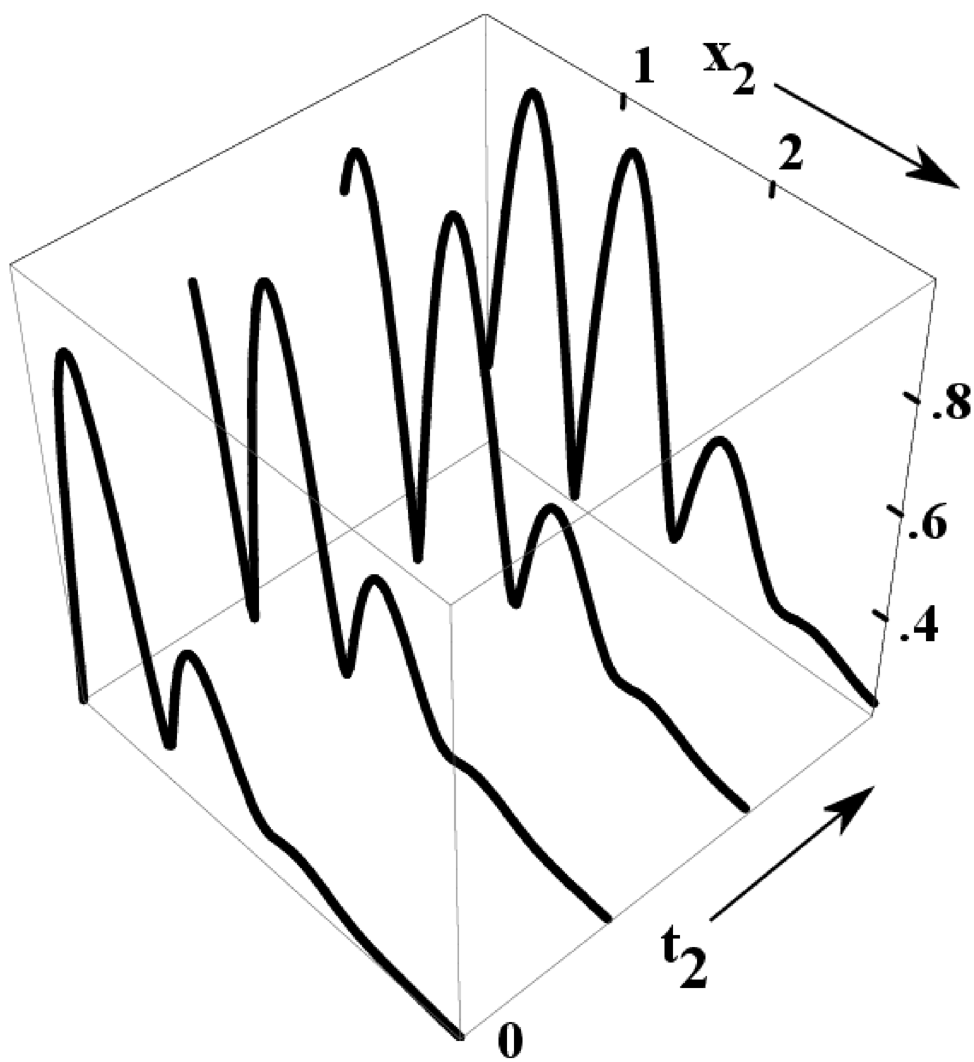

Figure 3.1: The "Doppler" shift is illustrated for $x_1 = 0$ and $t_1 = 0$ as a plot of the PDF vs. x_2 starting with $t_2 = 0$ (which is a slice of Figure 2.1) as the leftmost plot and then progressively increasing t_2 by 0.04τ in the plots toward the right.

The differences between simultaneous and non-simultaneous measurements of positions are a consequence of fixing terms in the phase which are proportional to t_1 while allowing the time evolution of terms proportional to t_2 until a measurement is made of the mirror position. To illustrate these differences, beyond that of the "Doppler" shift, two regimes are considered next. In regime A, measurement of the particle occurs in the space time region where the incident and reflected wavegroups do not overlap. In regime B measurement of the particle occurs in the spacetime region where the interference shown in Figure 2.1 occurs. In both regimes the constraints are: the measurement of the mirror occurs after that of the particle, the position measurements cannot determine directional motion, and once the particle has been measured no interaction occurs with the mirror since that would generate further correlations.

PDF results for regime A are shown as the dashed lines in Figure 3.2. At fixed values of $x_1 = 0, t_1 = \tau$, chosen so that the incident and reflected wavegroups do not overlap, there are three snapshots in $t_2 = (\tau, 2\tau, 3\tau)$ shown for the same particle and mirror parameters used in Figure 2.1. Since x_1, t_1 are fixed, these plots are related to slices of the PDF function shown in Figure 2.1 at fixed $x_1 = 0$ plotted along the x_2 coordinate for each snapshot at time t_2. For comparison, slices of Figure 2.1 for $x_1 = 0$ and $t_2 = t_1 = (\tau, 2\tau, 3\tau)$ are included in 2 as the solid lines. The dashed and solid lines therefore overlap for the $t_1 = \tau$ plot. The simultaneous PDF decays in time faster because now t_1 varies at fixed x_1, allowing the particle wavegroup substate to move away from x1 rather than having x_1 and t_1 fixed as it is in regime A.

PDF results for regime B are shown as the dashed lines in Figure 3.3 and Figure 3.4. At fixed values of $x_1 = 0, t_1 = 0$, chosen so that the incident and reflected wavegroups overlap when the particle is measured, there are three snapshots in $t_2 = (0, \tau, 2\tau)$ shown for the same particle and mirror parameters used in Figure 2.1 with the exception that in Figure 2.1 $M/m = 80$ (to simplify the interference pattern) while in Figure 3.4 $M/m = 3$ and $K/k = 6$. These plots are again related to slices of the PDF function shown in Figure 2.1 at fixed x_1

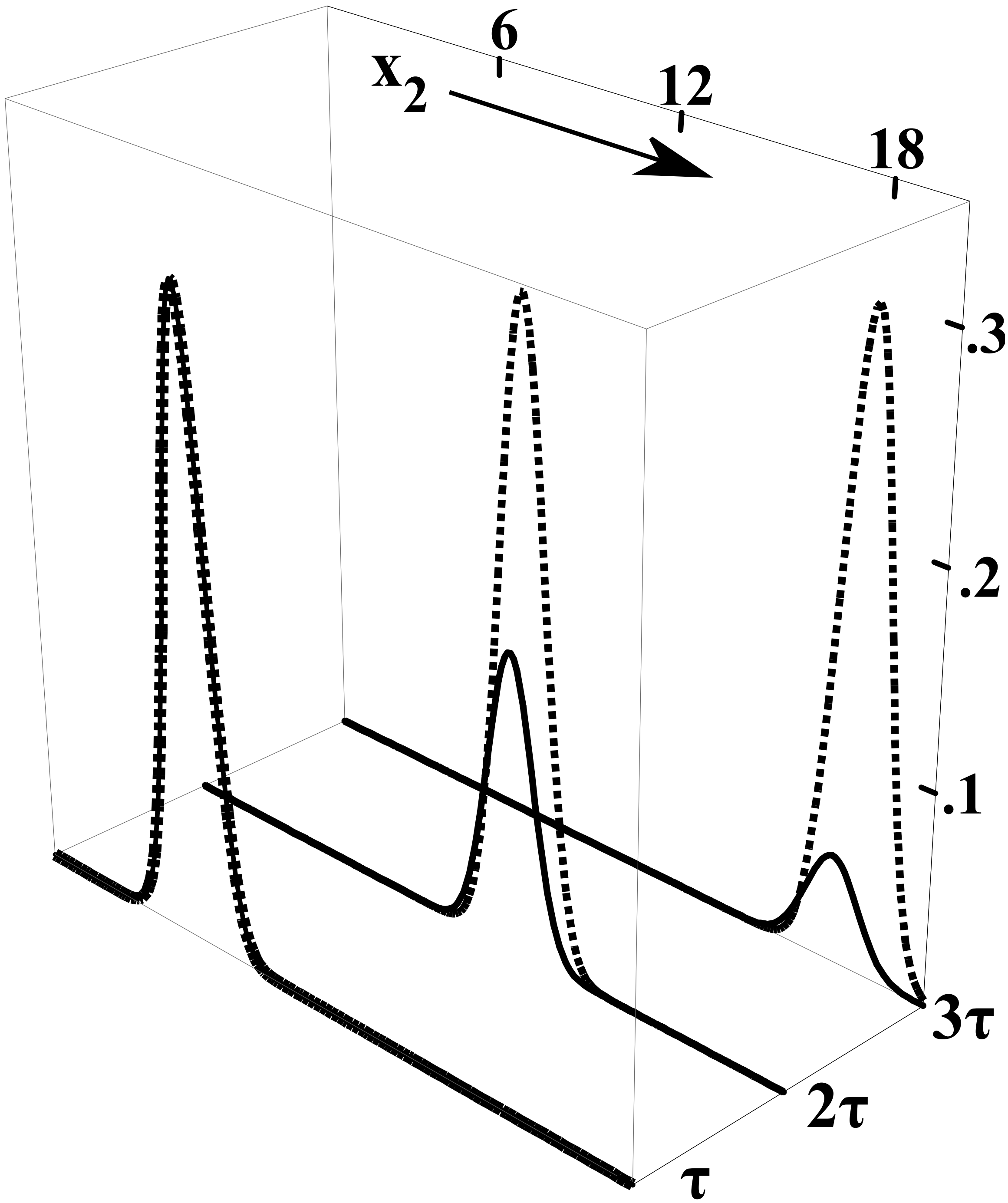

Figure 3.2: PDF plots for regime A (dashed lines) with $x_1 = 0, t_1 = \tau$ and *simultaneous* snapshots with $x_1 = 0, t_2 = t_1$ (solid lines) for sequential times $t_2 = (\tau, 2\tau, 3\tau)$ vs coordinate x_2.

plotted along the x_2 coordinate for each snapshot at times $t_2 = (0, \tau, 2\tau)$. Again, to directly relate these slices to Figure 2.1, figs. Figure 3.3 and Figure 3.4 also include the PDF results with the same value of $x_1 = 0$ for simultaneous measurements at times $t_2 = t_1 = (0, \tau, 2\tau)$ as the solid lines. The dashed and solid lines again overlap for the $t_2 = 0$ plot.

In Figure 3.3 the interference effects on the PDF continue well beyond the space time region of overlap for the incident and reflected wavegoups shown in Figure 2.1. This is most easily understood by considering the results shown in Figure 3.4 where the mirror's mass and wavevector are reduced by factors of 27 (resulting in a mirror mass three times larger than that of the particle) and 100 respectively. In regime B the particle position is measured in the space time interference region of Figure 2.1 but the direction of the particle is unknown. There are then two indistinguishable ways that the particle could have reached this position. It could have come from the incident or reflected particle wavegroup substates. This lack of knowledge about the particle is manifest in the mirror wavegroup substate which then consists of a superposition in which the mirror has yet to reflect and has already reflected the particle. These two mirror substates are spatially separated in Figure 3.4 while they overlap in Figure 3.3 (due to the more massive mirror) leading to the interference shown in Figure 3.3.

The bimodal PDF shown in Figure 3.4 disappears under simultaneous measurement for $t_1 = t_2 = (\tau, 2\tau)$ since at these times the incident and reflected wavegroups do not overlap (are at the upper snapshot of Figure 2.1 or beyond). A measurement of the particle at these space time points must then be associated with it having reflected from the mirror. Therefore only one mirror substate wavegroup exists and the mirror recoil causes this to coincide with the forward of two peaks shown in Figure 3.4.

While small coherence lengths make experimental verification of the predicitons in Figure 2.1 difficult, the results shown in Figure 3.1, Figure 3.3, and Figure 3.4 demonstrate the robust nature of the non-synchronous correlation (apart from decoherence effects). Experimental verification of such a correlation offers simplicity over that of a division of amplitude

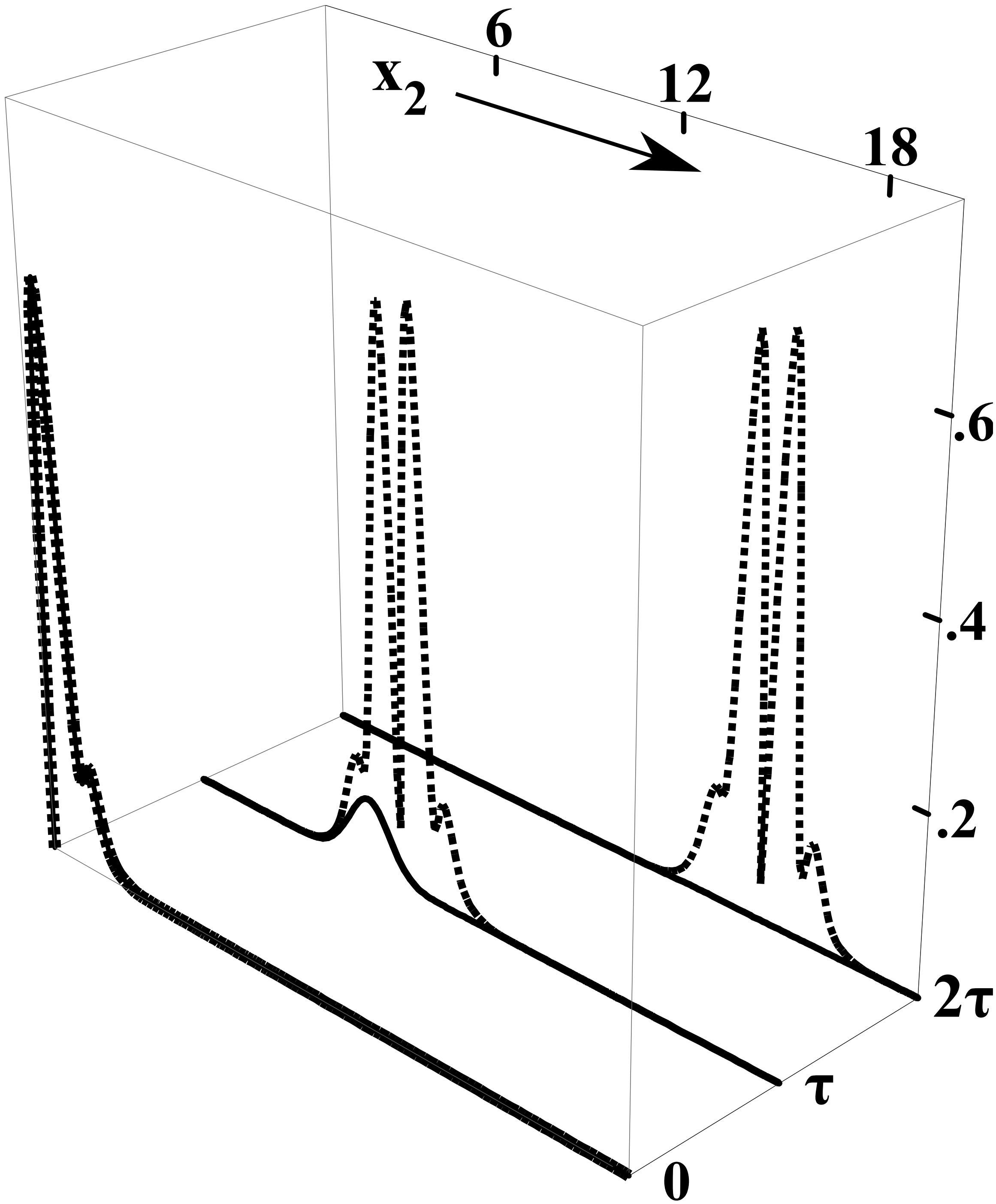

Figure 3.3: PDF plots for regime A (dashed lines) with $x_1 = 0, t_1 = 0$ and *simultaneous* snapshots with $x_1 = 0, t_2 = t_1$ (solid lines) for sequential times $t_2 = (0, \tau, 2\tau)$ vs coordinates x_2.

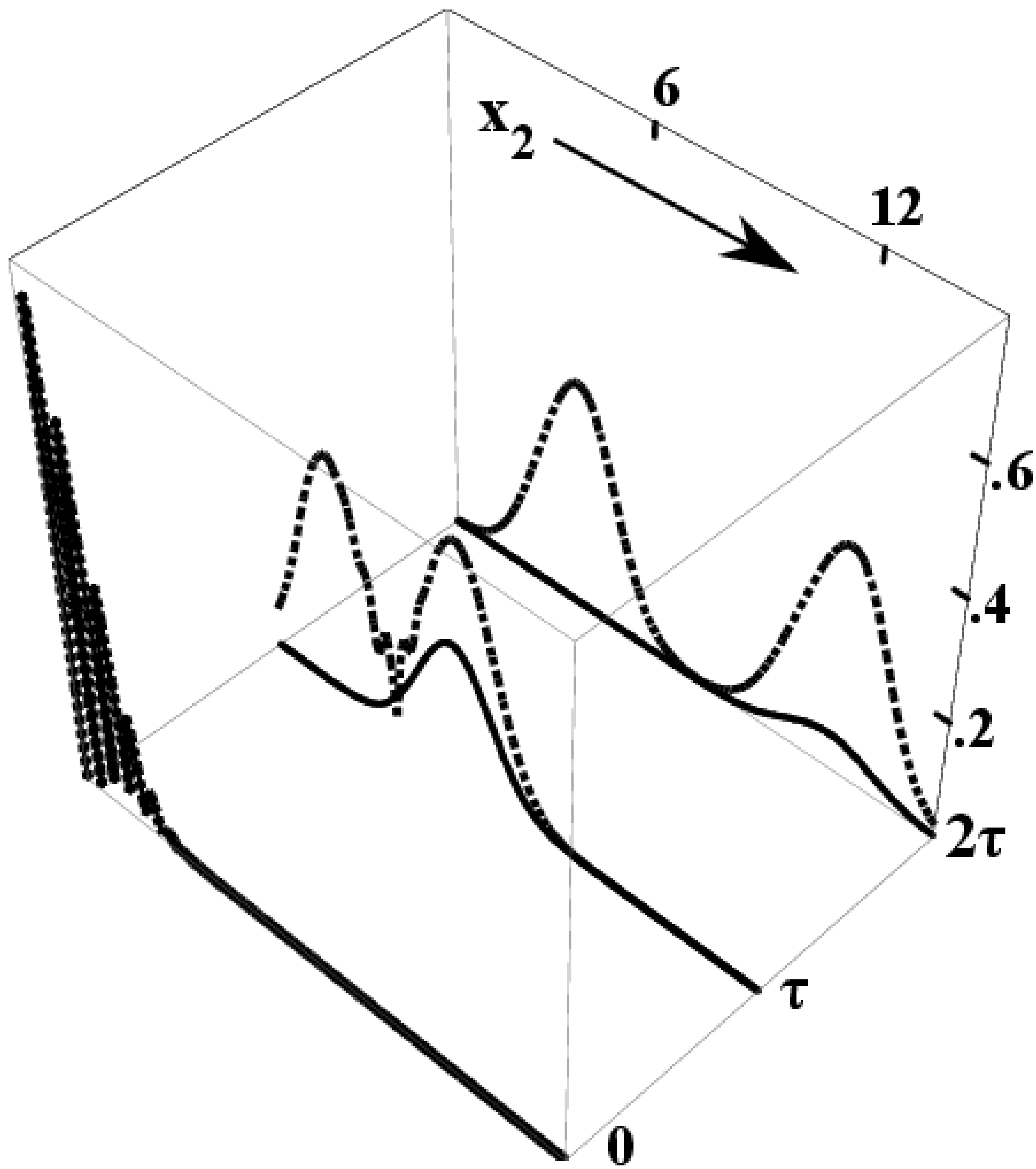

Figure 3.4: The same parameters as in Figure 3.3 except that the mirror's mass and wavevector are reduced by factors of 27 and 100 respectively.

or a division of wavefront interferometer where alignment and path differences need to be carefully matched for interference to be manifest.

Nevertheless, we consider next a division of amplitude interferometer in which two such particle-mirror correlated states are superposed. A simple example is in retro-reflection from each of the two surfaces of a moving slab, a realization of which is the neutron Fizeau effect.[22] Each weak surface reflection can be modeled as a delta function potential, both fixed to and symmetrically offset from the center of mass of the "slab" by distance D, with multiple reflections neglected. Modifying β to split rather than totally reflect the incident wave while including an offset in the delta function argument yields the two-particle reflected wavefunctions.

If the fringe visibility function for the resulting interference is non-zero, as it is when the reflected neutron substate wavegroups overlap, then the interference is determined predominately by a superposition of harmonic waves [23] (e.g. interference in 1 is determined predominately by Equation 3.9 when the wavegroups overlap). Narrow bandwidth wavegroups (where dispersion in reflection can be neglected), of spatial width w which satisfy $w >> D$, result in a constant two-particle reflected joint probability density $P \propto 4\sin^2[2DmM(V-v)/\hbar(m+M)]$. Observation of such a correlation is neither confined to the interaction region nor depends on a difference in the times of measurement of the particle and mirror since it is independent of spatial and temporal coordinates. To measure such an effect, the correlation must not decohere between the times of reflection and measurement. One-particle interference, obtained by averaging P over the slab's center of mass coordinate, does not eliminate the interference. A microscopic example is found in the Ramsauer effect where only the electron is measured.

In another example, a Mach-Zehnder neutron interferometer at rest [24] could have its two beam splitters and one mirror constructed from a single crystal of silicon (**MZM**) with the second mirror detached (**DM**). In a simple 1-D model of the resulting interference, the neutron which is split at the input port could either become correlated with the center of mass of **MZM** along one path or with the center of mass of **DM** along the other. A correlated particle-mirror state describes each path yet their superposition results in a three particle state since the neutron is common to the two interfering states. Destructive interference is then manifest in no observation of the neutron at the interferometer output port coincident with no observation at particular center of mass locations of **MZM** and **DM**. There is now a large spatial separation between the three apparatus needed to simultaneously measure the neutron at the output port and the center of mass locations of **MZM** and **DM**. However, the fringe spacing now depends not only on the difference in particle phases along the two paths but also differences in phases associated with **DM** and **MZM**. Unless these macroscopic "mirrors" move at small speeds, the interference fringes are imperceptible due to these large mirror masses. If **MZM** and **DM** are attached to each other (share a common center of mass), and their center of mass is not measured then this yields the expected one-particle neutron interference.

We have shown that reflection of a microscopic particle from a macroscopic mirror leads to correlated particle-mirror interference effects which are essentially determined by the mass of the microscopic particle and result in fringe spacings for the mirror which are enhanced in comparison with that of one-particle interference. A mechanism for transferring coherence from the particle to the mirror has also been presented. Some issues of implementation have been discussed including the superposition of multiple two-particle state reflections to generate spatially separated interference in the correlation of particle-mirror positions. These results, although far from being comprehensive, indicate a potential direction for further research in extending the quantum-classical boundary to larger masses.

CHAPTER 4
CONCLUSION

Considering only the case of simultaneous measurement, two important features result. First, we see robust interference effects in the correlated measurement of the position of the particle and the position of the mirror. The interference effects seen in this simple system are not dependent on division of amplitude or division of wavefronts. Thus path lengths do not need to be matched, nor are there alignment issues.

The fringe spacing of the interference of the mirror with itself in the macroscopic limit is dependent inversely on the mass of the particle reflecting from the mirror, but not on the mass of the mirror itself. This sits in contrast to double slit interferometers, where the fringe spacing is always inversely dependent on the mass of the interfering particle.

The second important feature of the case of simultaneous measurement is coherence transfer due to reflection. The reflection of the particle from the mirror results in a reciprocal transfer of coherence between the particle and the mirror. This is consistent with the notion of wave-particle duality manifested in elastic collisions.

In order to better analyze the system by allowing non-simultaneous measurements, we need to extend our mathematical machinery. By extending our tools by adding in multiple time parameters to Schrödinger's equation, we were able to examine the system with non-simultaneous measurements while deriving a doppler shift for both the particle and the mirror from which it reflects.

REFERENCES CITED

[1] E Schrödinger. Naturwissenschaften 23 807 schrödinger e 1935. *Naturwissenschaften*, 23(823):152, 1935.

[2] A. Einstein, B. Podolsky, and N. Rosen. Can quantum-mechanical description of physical reality be considered complete? *Phys. Rev.*, 47:777–780, May 1935. doi: 10.1103/PhysRev.47.777. URL `http://link.aps.org/doi/10.1103/PhysRev.47.777`.

[3] N Bohr, JA Wheeler, and WH Zurek. Quantum theory and measurement, 1983.

[4] Anthony J Leggett. Testing the limits of quantum mechanics: motivation, state of play, prospects. *Journal of Physics: Condensed Matter*, 14(15):R415, 2002.

[5] Roger Penrose. On gravity's role in quantum state reduction. *General relativity and gravitation*, 28(5):581–600, 1996.

[6] Florian Fröwis and Wolfgang Dür. Measures of macroscopicity for quantum spin systems. *New Journal of Physics*, 14(9):093039, 2012.

[7] Amit Hagar. Decoherence. *Philosophical Transactions of the Royal Society A: Mathematical, Physical and Engineering Sciences*, 370(1975):4425–4428, 2012.

[8] C Monroe, DM Meekhof, BE King, DJ Wineland, et al. A" schrödinger cat" superposition state of an atom. *SCIENCE-NEW YORK THEN WASHINGTON-*, pages 1131–1135, 1996.

[9] Caspar H Van Der Wal, ACJ Ter Haar, FK Wilhelm, RN Schouten, CJPM Harmans, TP Orlando, Seth Lloyd, and JE Mooij. Quantum superposition of macroscopic persistent-current states. *Science*, 290(5492):773–777, 2000.

[10] Alexander D Cronin, Jörg Schmiedmayer, and David E Pritchard. Optics and interferometry with atoms and molecules. *Reviews of Modern Physics*, 81(3):1051, 2009.

[11] B Abbott, R Abbott, R Adhikari, P Ajith, B Allen, G Allen, R Amin, SB Anderson, WG Anderson, MA Arain, et al. Observation of a kilogram-scale oscillator near its quantum ground state. *New Journal of Physics*, 11(7):073032, 2009.

[12] Markus Aspelmeyer, Pierre Meystre, and Keith Schwab. Quantum optomechanics. *Physics Today*, 65(7):29–35, 2012.

[13] Tobias J Kippenberg and Kerry J Vahala. Cavity optomechanics: back-action at the mesoscale. *science*, 321(5893):1172–1176, 2008.

[14] CA Regal and KW Lehnert. From cavity electromechanics to cavity optomechanics. In *Journal of Physics: Conference Series*, volume 264, page 012025. IOP Publishing, 2011.

[15] Aaron D OConnell, M Hofheinz, M Ansmann, Radoslaw C Bialczak, M Lenander, Erik Lucero, M Neeley, D Sank, H Wang, M Weides, et al. Quantum ground state and single-phonon control of a mechanical resonator. *Nature*, 464(7289):697–703, 2010.

[16] A Nunnenkamp, K Børkje, and SM Girvin. Single-photon optomechanics. *Physical Review Letters*, 107(6):63602, 2011.

[17] Francesco De Martini, Fabio Sciarrino, Chiara Vitelli, and Francesco S Cataliotti. Coherent scattering of a multiphoton quantum superposition by a mirror bec. *Physical review letters*, 104(5):50403, 2010.

[18] Otto Wiener. Stehende lichtwellen und die schwingungsrichtung polarisirten lichtes. *Annalen der Physik*, 276(6):203–243, 1890.

[19] Kurt Gottfried. Two-particle interference. *American Journal of Physics*, 68:143, 2000.

[20] Paolo Tommasini, Eddy Timmermans, and A. F. R. de Toledo Piza. The hydrogen atom as an entangled electron–proton system. *American Journal of Physics*, 66(10):881–886, 1998. doi: 10.1119/1.18977. URL `http://link.aip.org/link/?AJP/66/881/1`.

[21] J. H. McGuire and A. L. Godunov. Time evolution and use of multiple times in the N -body problem. *Phys. Rev. A*, 67:042701, Apr 2003. doi: 10.1103/PhysRevA.67.042701. URL `http://link.aps.org/doi/10.1103/PhysRevA.67.042701`.

[22] Ulrich Bonse and Andreas Rumpf. Interferometric measurement of neutron fizeau effect. *Physical review letters*, 56(23):2441–2444, 1986.

[23] WA Hamilton, AG Klein, and GI Opat. Longitudinal coherence and interferometry in dispersive media. *Physical Review A*, 28(5):3149, 1983.

[24] H Rauch, W Treimer, and U Bonse. Test of a single crystal neutron interferometer. *Physics Letters A*, 47(5):369–371, 1974.